

Investigation of the single-spring lattice model in simulation of 2D solid problems by DEM

V. Vadluga*, R. Kačianauskas**

*Vilnius Gediminas Technical University, Saulėtekio al.11, 10223 Vilnius-40, Lithuania, E-mail: vvad@fm.vtu.lt

**Vilnius Gediminas Technical University, Saulėtekio al.11, 10223 Vilnius-40, Lithuania, E-mail: rkac@fm.vtu.lt

1. Introduction

In the last four decades, the Finite Element Method (FEM) was the most popular numerical technology used in mechanical analysis of various solids and engineering structures. Recently, the Discrete Element Method (DEM) has opened new vistas for numerical simulation of dynamic behaviour.

A concept of the discrete, originally distinct, element method is referred basically to the original work of Cundall and Strack [1]. It was aimed to describe mechanical behaviour of granular assemblies composed of discrete elements, i.e. discs, and (later) spheres, in particular.

The main difference between both FEM and DEM lies in a different space discretisation concept. FEM operates upon assemblies of finite elements, while discrete parameters are attached to nodal points located within a continuous element. An algebraic model deals simultaneously with all elements covering the entire solution domain. Time tracking of dynamic processes and a rapid change of the structure's geometry and topology presents additional difficulties.

DEM operates on the basis of the single-point approach. A discrete element is considered separately and presents a material particle with the prescribed characteristics, where all parameters are associated with the centre of the particle.

A particular state of an individual DEM is assumed to be time-dependent, while tracking of particle temporal behaviour is the main goal of any DEM simulation. Tracing of each particle in time is defined by dynamic equilibrium of forces acting on the particle and described by a system of fully deterministic equations of motion of classical mechanics. A large number of particles as well as time integration steps and variable topology are essential attributes of DEM. Application of DEM for brittle cracking of solids characterized by shock type behaviour appears to be area of numerical simulation.

Careful interpretation of the DEM and its comparison with FEM showed not only external differences, but some conceptual similarities as well. Inter-particle forces may be interpreted as internal forces of continuum in terms of network forces, where the network line is considered as one-dimensional FE. Therefore, this analogy was elaborated for the application of DEM for discretisation of structures and solids.

The simplest DEM approach is merely a modification of structural analysis. A particular contribution presented in the earlier work of Kawai [2] could be mentioned in this respect. A short review of this approach and its application to the nonlinear static analysis of plane framed structures is presented by [3, 4].

Different approaches and methodologies applied to the analyses of homogeneous and heterogeneous solids appeared during the past decade. A concept of the particulate media composed by polygonal particles prevailed in the work of D'Addetta and Ramm [5]. There, an interface enhanced FEM methodology was introduced and combined with the particle methodology. Interface elements comprise a fixed number of normal and tangential spring sets being directly defined at the particle edges. A combination of discs and hexagonal DE for fracture of rock is developed by [6].

Straightforward application of the standard DEM to fracture of sandstone is presented by [7]. Poly-dispersed assembly of conventional spherical particles with normal and tangential contact was applied to the modelling of concrete [8, 9] or agglomerates [10].

Here, the characteristics of the connection element are chosen experimentally.

Generally, discretisation of solids by DEM employs a particle-network concept. An approach which allows a straightforward application of the spring-force concept to continua is also called lattice-type model. A number of modifications of connection elements between the nodes of the lattice grid, exploring beam analogy, have been suggested. The rods or springs which are the simplest elements described by the nodal translation displacements are compatible, however, with classical continuum theories. Brittle fracture and dynamic post-fracture behaviour of 1D continuum was considered by [11], where the influence of space discretisation as well as the effect of damping and local nonlinearity were investigated. The simplest truss analogy was also extended to 2D problems in [12]. There, additional calibration of the spring stiffness was performed from the comparison with the FEM simulations.

The application of shear elements [13] and Euler-Bernoulli beam elements described in terms of rotation DOF [14, 15] would require the higher order continuum models.

Some attempts have been made to develop continuum-based lattice models for DEM. Normal and tangential spring stiffness for 2D hexagonal lattice in the plane stress and plane strain problem without theoretical explanation was considered by Savamoto et al. [16]. Probably, the first most comprehensive study of this type was published by Mustoe [17] and Griffiths and Mustoe [18]. They introduced the one-dimensional element comprising axial and shear deformation modes. Both plane strain and plane stress examples were presented and good agreement between displacements obtained from the discrete element formulation and analytical and/or solid finite element solutions was observed. The dependence on grid geometry and Poisson's ratio was also found. However, from the theo-

retical point of view, the presence of shear stiffness was hardly compatible with the classical elasticity theory.

This energy-based deformation methodology was later extended for 2D hexagonal and square lattice [19], including anisotropy as applied by [20], while for cubic lattice it was used by [21]. There, the hybrid DEM/FEM model, increasing the domain of application of the particle models, and extending the possibilities of calibration/development of DEM was proposed and the approach similar to that applied to fracture analysis was given in [22].

The present paper addresses a single axial spring-based lattice model applied to the build-up of DEM. The Poisson's ratio dependent stiffness parameter of the spring compatible with continuum displacement field was derived by applying virtual work principle. Consistency of the approach was considered by solving dynamic problems and comparison with FEM simulations. The application for the simulation of brittle fracture is also presented.

The paper is arranged as follows. Computational methodology is presented in Section 2. Derivation of the single-spring stiffness is described in Section 3. Validation examples are given in Section 4. The application for simulation of brittle fracture during compression is illustrated in Section 5, while conclusions are given in Section 6.

2. Computational methodology

General statements. The time-driven DEM is applied to the simulation of dynamic behaviour of the elastic two-dimensional solid. Actually, the present work is restricted to the plane stress problem, but the extension to plane strain would be a rather formal task. Consequently, the plate of constant thickness s is regarded here as two-dimensional solid. It is subjected to in plane loads attached to the middle plane. The solid is considered in plane Oxy of the Cartesian co-ordinates, while axis Oz points thickness direction.

Generally, elasticity properties of solids are defined by elasticity tensor and may be described in terms of 3×3 -order elasticity matrix. In the case of an isotropic material, the elasticity properties are defined by elasticity modulus E and Poisson's ratio ν . Density of the material is characterised by ρ . If the material is assumed to be heterogeneous, the material constants may be defined as position $\mathbf{x} = \{x, y\}^T$ dependent variables.

Discretisation approach. The DEM discretisation approach relies on the concept applied to the description of granular material. The 2D solid is regarded as a system of the finite number N of deformable material particles i ($i = 1, \dots, N$).

The discrete model is implemented by covering a computational domain with the hexagonal lattice grid. The lattice is constructed by equilateral triangles (Fig. 1, a). Each particle i represents a hexagon composed of six equal triangles. The hexagon encompasses a half of each connection line. The location of the particle coincides with the lattice node and is defined by the global co-ordinates $\mathbf{x}_i = \{x_i, y_i\}^T$, while the geometry of the particle is defined by a characteristic dimension L of the grid.

The density of the material is constant within the particle and is assumed to be constant ρ_i . Mass of the solid is described by a set of lumped masses m_i , concentrated in the centres of particles.

Generally, lattice concept replaces continuum by discrete network of single bars or springs. The discrete model is just fictitious-imaginary model has to be energy-equivalent to continuum. Real interparticle contact is here not considered and is simple replaced by equilibrium of selected nodes.

Consequently, the interaction of particles i and j is described by the connection element $i-j$. The connection element presents a line segment of the lattice grid. Constitutive properties of the solid are assigned to particular lines. The connection element may generally reflect a highly complicated model of continuum, including non-linearity, time-dependence, degradation, etc. It should be noted, that a definition and explicit characterisation of the discrete elasticity parameters presents the key issue of the DEM simulations.

The developed DEM approach assumes a description of the discrete model by applying the single normally deformed spring (Fig. 1, b). The suggested element may be easily extended by adding damping or fracture properties.

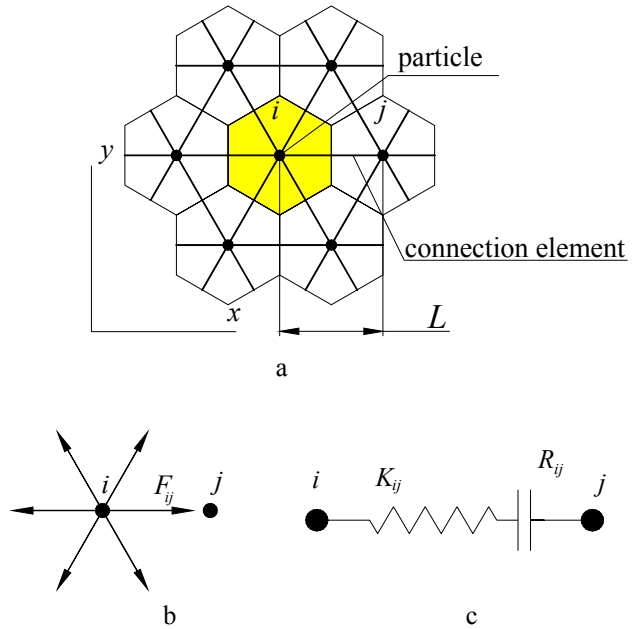


Fig. 1 Illustration of discrete model: a – a fragment of the lattice; b – inter-particle forces of particle i ; c – a model of the connection element $i-j$

Governing equations. DEM is a numerical technique aimed at tracking the dynamic behaviour of individual particles with their mass, geometry and constitutive properties. Governing equations present dynamic equilibrium, or motion, of all material particles. They are defined for each individual particle and considered separately.

Generally, governing equations are presented by a traditional DEM approach used for the simulation of granular materials [1, 23, 24] described in work [11]. The motion of particle i in time t is considered by applying the Newton's second law.

In terms of continuum mechanics, a motion of the material particle of the two-dimensional solid is characterised by two independent translations, therefore, two equations of translation, or dynamic equilibrium, expressed in terms of the forces acting at the centre of the particle, are as follows

$$m_i \frac{d^2 \mathbf{x}_i(t)}{dt^2} = \mathbf{F}_i(t) \quad (1)$$

where

$$m_i = \frac{\sqrt{3}}{2} L^2 \delta \rho \quad (2)$$

is the mass of hexagonal particle, while the vector $\mathbf{F}_i = \{F_{ix}, F_{iy}\}^T$

$$\mathbf{F}_i = \mathbf{F}_{i,ext} + \sum_{j=1}^6 \mathbf{F}_{ij} \quad (3)$$

presents the resultant of all external $\mathbf{F}_{i,ext}$ and particle interaction forces. Intersparticle forces \mathbf{F}_{ij} , acting on the particle i , are illustrated in Fig. 1, b. Hereafter, a subscript j denotes six neighbouring particles.

Hence, the intersparticle force vector \mathbf{F}_{ij} is actually composed of normal forces acting along the connection line and defined in local co-ordinates attached to the grid line. Their explicit evaluation by using the single spring approach will be presented below.

Time integration. The motion of each particle i , or, more definitely, tracking of its position $\mathbf{x}_i(t)$, velocity $\mathbf{v}_i(t) \equiv \dot{\mathbf{x}}_i(t)$ and acceleration $\mathbf{a}_i(t) \equiv \ddot{\mathbf{x}}_i(t)$ in time t is performed by using the Eq. (1).

The incremental approach is used for time integration of the equation of motion, while the explicit time integration schemes present the most proper technique used in DEM. The Verlet velocity algorithm is currently applied to integration [23].

Implementation. The DEM approach described above was implemented into the original software code. The code presents a modified version of the DEM code DEMMAT developed in the Laboratory of Numerical Modelling of Vilnius Gediminas Technical University, see [24, 25].

3. A single-spring model

The suggested continuum consistent single-spring lattice model manifests that all intersparticle forces $F_{ij} \equiv F_{el,ij}$ in expression (3) are elastic forces defined by a single elasticity constant, more precisely, by axial stiffness K_{ij} of the intersparticle spring. The single-spring model assumes additionally equality of all springs, thus, $K_{ij} = K$. Consequently, the local constitutive relationship is assumed to be linear and is defined as

$$F_{ij} = K h_{ij} \quad (4)$$

where, h_{ij} presents intersparticle displacement as elongation of the connection line $i-j$

$$h_{ij} = u_{nj} - u_{ni} \quad (5)$$

being expressed in terms of the local longitudinal displacements u_i and u_j of the connected nodes i and j of the grid.

Continuum-consistent single-spring elasticity constant K will be derived by applying the principle of the virtual work.

Let us consider two-dimensional linear elastic continuum. Restricting ourselves to the plane stress problem we analyze the continuum presenting a plate of thickness s . A constitutive relationship between stresses $\boldsymbol{\sigma} = \{\sigma_{11}, \sigma_{22}, \tau_{12}\}^T$ and strains $\boldsymbol{\varepsilon} = \{\varepsilon_{11}, \varepsilon_{22}, \gamma_{12}\}^T$

$$\boldsymbol{\sigma} = [\mathbf{D}_C] \boldsymbol{\varepsilon} \quad (6)$$

is defined by the symmetric elasticity matrix

$$[\mathbf{D}_C] = \begin{bmatrix} d_{C11} & d_{C12} & 0 \\ d_{C12} & d_{C22} & 0 \\ 0 & 0 & d_{C33} \end{bmatrix}$$

where

$$d_{C11} = d_{C22} = \frac{E}{1-\nu^2}, \quad d_{C12} = \frac{\nu E}{1-\nu^2} \quad (7)$$

$$d_{C33} = \frac{E}{2(1+\nu)}$$

Assuming the virtual displacement approach, virtual work $\delta U_C \equiv \delta U_C(\mathbf{x}_i)$ done by the virtual strains $\delta \boldsymbol{\varepsilon} \equiv \delta \boldsymbol{\varepsilon}(\mathbf{x}_i)$ in the point \mathbf{x}_i of continuum reads as

$$\delta U_C = (\boldsymbol{\varepsilon})^T [\mathbf{D}_C] \delta \boldsymbol{\varepsilon} \quad (8)$$

Explicitly,

$$\delta U_C = d_{C11} \varepsilon_{11} \delta \varepsilon_{11} + d_{C22} \varepsilon_{22} \delta \varepsilon_{22} + d_{C12} \varepsilon_{11} \delta \varepsilon_{22} + d_{C12} \varepsilon_{22} \delta \varepsilon_{11} + d_{C33} \gamma_{12} \delta \gamma_{12} \quad (9)$$

The elastic virtual work δU_{Di} for a discrete particle i imposed by virtual interaction with neighbouring particles may be presented in terms of normal forces and elongations of springs. Taking into account the Eqs. (4)-(5) it may be defined as

$$\delta U_{Di} = \sum_{j=1}^p \frac{1}{2} K h_{ij} \delta h_{ij} \quad (10)$$

The factor $\frac{1}{2}$ indicates that only half of the deformation work of spring ij is assigned to particle i .

Looking for analogy with continuum model (8), the equivalent discrete specific virtual work is suggested by averaging of (10) over the volume of particle V_i

$$U_D = \frac{1}{V_i} U_{Di} \quad (11)$$

where particle volume (Fig. 1, a) is expressed as

$$V_i = tA_i = \frac{\sqrt{3}}{2} L^2 s \quad (12)$$

The normal local displacement u_{ni} or u_{nj} of particles i or j may be expressed in terms of the global displacements $\mathbf{u}_i = \{u_{ix}, u_{iy}\}^T$ and the direction matrix $[\mathbf{n}_{ij}]$, respectively, as

$$\mathbf{u}_{n_i} = [\mathbf{n}_{ij}]^T \mathbf{u}_i, \quad \mathbf{u}_{n_j} = [\mathbf{n}_{ij}]^T \mathbf{u}_j \quad (13)$$

Denoting cosines of the normal and tangential directions of spring i - j by n_{xij} and n_{yij} , the direction matrix may be defined as $[\mathbf{n}_{ij}] = \begin{bmatrix} n_{xij} \\ n_{yij} \end{bmatrix}$.

Referring to Fig. 1, b, six direction matrices of the lattice grid may be defined as

$$\begin{aligned} [\mathbf{n}_{i1}] &= \begin{bmatrix} 1 \\ 0 \end{bmatrix}, \quad [\mathbf{n}_{i2}] = \begin{bmatrix} \frac{1}{2} \\ \frac{2}{\sqrt{3}} \end{bmatrix}, \quad [\mathbf{n}_{i3}] = \begin{bmatrix} -\frac{1}{2} \\ \frac{2}{\sqrt{3}} \end{bmatrix}, \\ [\mathbf{n}_{i4}] &= \begin{bmatrix} -1 \\ 0 \end{bmatrix}, \quad [\mathbf{n}_{i5}] = \begin{bmatrix} -\frac{1}{2} \\ -\frac{2}{\sqrt{3}} \end{bmatrix}, \quad [\mathbf{n}_{i6}] = \begin{bmatrix} \frac{1}{2} \\ -\frac{2}{\sqrt{3}} \end{bmatrix} \end{aligned} \quad (14)$$

Defining the global interaction displacements $\Delta \mathbf{u}_{ij} = \{u_{jx} - u_{ix}, u_{jy} - u_{iy}\}^T$, they may be expressed in terms of strains and the geometric matrix $[\mathbf{B}_{ij}]$ in this way

$$\Delta \mathbf{u}_{ij} = [\mathbf{B}_{ij}] \boldsymbol{\varepsilon}_{ij} \quad (15)$$

Assuming small rotations, the influence of shear strain was neglected, while the geometric matrix was simplified

$$[\mathbf{B}_{ij}] = \begin{bmatrix} x_j - x_i & 0 \\ 0 & y_j - y_i \end{bmatrix}$$

By making simple manipulations, we may express it in terms of interparticle distance L_{ij} and direction cosines $[\mathbf{n}_{ij}]$.

$$[\mathbf{B}_{ij}] = L \begin{bmatrix} n_{xij} & 0 \\ 0 & n_{yij} \end{bmatrix} \quad (16)$$

Taking into account the transformations (13) and (15), the discrete virtual work, the expression (11) may be presented in the form of continuum.

$$\delta U_D = (\boldsymbol{\varepsilon})^T [\mathbf{D}_D] \delta \boldsymbol{\varepsilon} \quad (17)$$

where, the discrete elasticity matrix is as follows

$$[\mathbf{D}_D] = \frac{1}{2} \frac{L^2}{V_i} K \sum_{j=1}^p [\mathbf{B}_{ij}]^T [\mathbf{n}_{ij}] [\mathbf{n}_{ij}]^T [\mathbf{B}_{ij}] \quad (18)$$

Actually, (18) reads

$$[\mathbf{D}_D] = \begin{bmatrix} d_{D11} & d_{D12} & 0 \\ d_{D12} & d_{D22} & 0 \\ 0 & 0 & 0 \end{bmatrix}$$

Substituting of Eqs. (12), (14) and (17) into Eq. (18), yields explicitly

$$d_{D11} = d_{D22} = \frac{\sqrt{3}K}{4s}, \quad d_{D12} = \frac{\sqrt{3}K}{4s} \quad (19)$$

The equality of continuous and discrete virtual works

$$\delta U_D = \delta U_C \quad (20)$$

or, more precisely, of the elasticity matrices

$$[\mathbf{D}_D] = [\mathbf{D}_C] \quad (21)$$

provides the necessary conditions for evaluating of spring stiffness.

However, the derivation of the spring model is not a formal and simple task because it requires physical as well as mathematical consistency of both continuous and discrete approaches. Consequently, the number of unknowns has to be equal to the number of equations. In this case, apart from the ignoring of the shear strain term, we have a single-spring constant and two equations.

Application of the equality $d_{D11} = d_{C11}$ yields the expression

$$K_1 = \frac{4\sqrt{3}Es}{9(1-\nu^2)} \approx \frac{0,7698Es}{1-\nu^2} \quad (22)$$

Application of the equality $d_{D12} = d_{C12}$ yields the expression

$$K_2 = \frac{4\nu Es}{\sqrt{3}(1-\nu^2)} \approx 2,3094 \frac{\nu}{1-\nu^2} Es \quad (23)$$

The equality of both solutions is achieved, when the value $\nu = 0.33$. A peculiarity of this specific point was already indicated by two-parameter solution of in [16, 17, 19], when considering normal stiffness K_{Gn} , K_{Gs}

$$\begin{aligned} K_{Gn} &= \frac{Es}{\sqrt{3}(1-\nu)} \\ K_{Gs} &= \frac{E(1-3\nu)s}{\sqrt{3}(1-\nu^2)} \end{aligned} \quad (24)$$

The obtained stiffness presents Poisson's ratio dependent parameters, while the variations are depicted in Fig. 2.

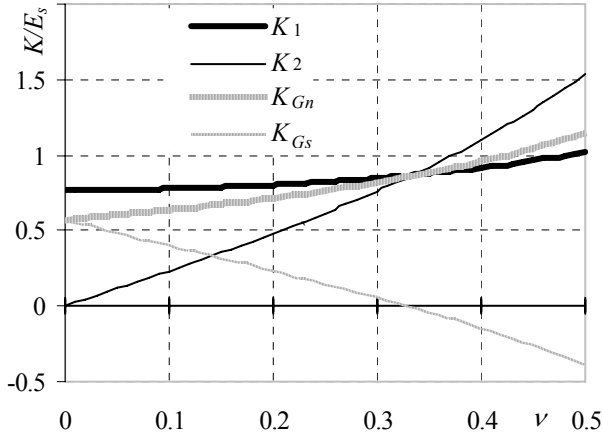


Fig. 2 Variation of stiffness parameters against the Poisson's ratio

Graphs in Fig. 2 clearly exhibit the equality of all expressions for K_1 , K_2 and K_{Gn} , as well as indicate zero value of shear stiffness K_{Gs} .

Considering the above results, it may be stated that single-spring model is physically and mathematically consistent only for Poisson's ratio $\nu = 0.33$, while the validity of the model in the vicinity of this point would be checked by numerical experiments.

4. Investigation of deformation behaviour

The performance of the developed single-spring lattice model was examined by considering elastodynamic deformation behaviour. The spring stiffness (22) was implemented into DEMMAT code and applied to simulation problems.

The two-dimensional rectangular solid domain was considered as a representative example. The geometry of the domain is defined by two characteristic dimensions $H = 400$ mm and $B = 100$ mm (Fig. 3). Actually, the domain may be treated as in-plane loaded thin plate, while thickness $s = 10$ mm is prescribed.

The plate boundaries AB and CD are assumed to be connected to rigid walls, while AC and BD are free boundaries. The external compressing loading is implemented via the displacement of boundary CD, i.e. $u(t)$, thus, loading is defined as a time-dependent phenomenon controlled by the prescribed displacement $u(t) = 0 \div 2.0$ mm (at constant velocity $v_{CD}(t) = 1$ m/s).

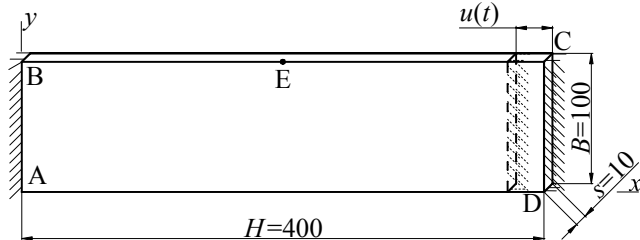


Fig. 3 Geometry of the plate with boundary conditions and loading

An elastic material is characterized by the following properties. Density of the material is $\rho = 2500$ kg/m³, while its modulus of elasticity $E = 17.1$ GPa.

The numerical analysis was made in the following manner. The rectangular domain was covered by a hexagonal lattice. The lattice grid serves as the base for both DEM and FEM models. The DEM model is developed according to the described methodology, while the FEM presents an assembly of linear triangular elements.

The lattice grid, having a characteristic dimension $L_{ij} = H/n_x = 400/126 = 3.175$ mm (here, n_x is the number of subdivisions along x axis), has been employed. The DEM model contains 13717 connection elements and 4681 particles with 9362 degrees of freedom. It should be noted that the geometry of interacting particles at the boundary is slightly modified.

The FEM model contains 9072 triangular elements with the same number of nodes and degrees of freedom. The finite element analysis is performed using ANSYS software [26].

The loading for both models is implemented in $g = 44069$ time steps with time increment $\Delta t = 4.538 \cdot 10^{-8}$ s.

Two representative variables - longitudinal u_E and transversal displacement q_E of the mid-side point E are examined in detail. The emphasis is on the evaluation of the influence of Poisson's ratio ν .

Simulation results obtained by both DEM and FEM for different ν values in the form of time histories are depicted in Fig. 4.

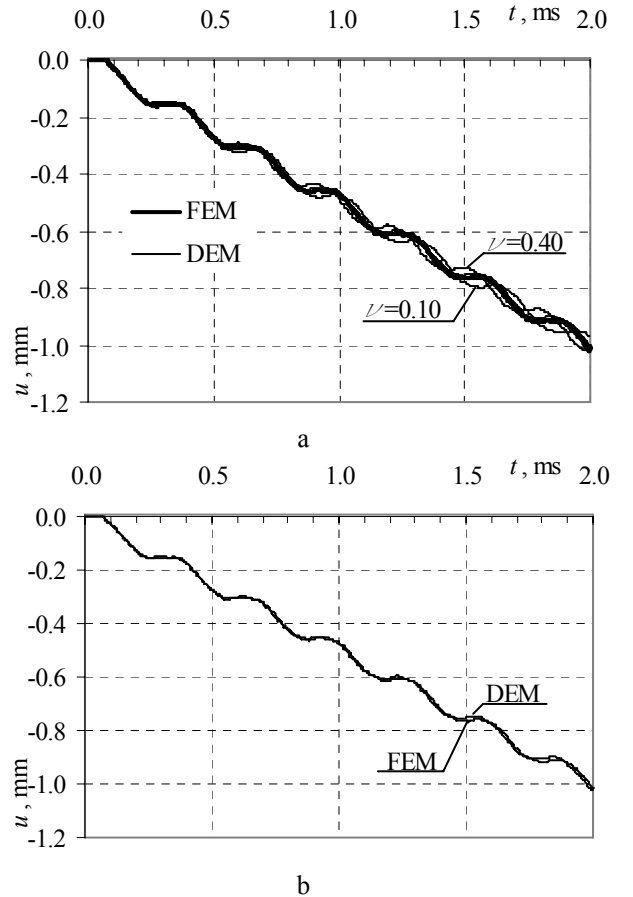


Fig. 4 Time histories of longitudinal displacement u_E for various ν : a - $\nu = 0.10; 0.20; 0.30; 0.33; 0.40$ b - $\nu = 0.33$

Time histories of the longitudinal displacement q_E obtained for various ν values ranging between 0.1 and 0.4, are plotted in Fig. 4. The illustration is restricted to a short

loading period, where $u_{CD}=2.00$ mm. The FEM results illustrated by curves are practically insensitive to Poisson's ratio. It could be observed from the graph that DEM results yield more extensive variation. It is confirmed that both methods provide the identical results, when $\nu=0.33$ (Fig. 4, b).

Here, the variation of the average values is plotted against Poisson's ratio. Higher sensitivity of the DEM results can be clearly seen, however, the difference between the approximated DEM and "exact" FEM results (Fig. 5) varies in the range 3-5 %.

It can be concluded that the suggested single-spring model is able to capture longitudinal deformation behavior.

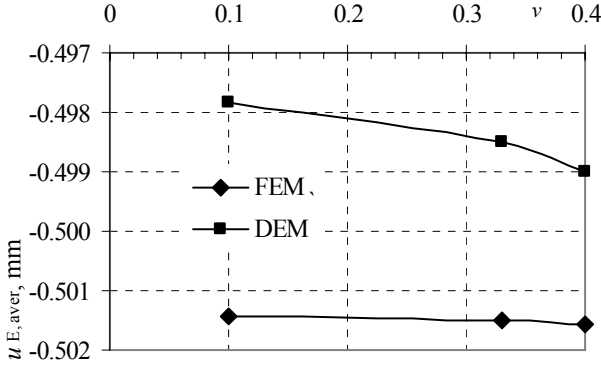


Fig. 5 Variation of average longitudinal displacements against Poisson's ratio

A transversal displacement of the point E is considered in the same manner. Time histories are plotted in Fig. 6.

It could be stated that FEM results show the same order of sensitivity as that observed for longitudinal displacement, while DEM results exhibited considerable scattering. The variation of displacements against Poisson's ratio is plotted in Fig. 7.

Considering the above graph, we can see that the DEM results are accurate for $\nu=0.33$, while being dramatically diverging for other values. Thus, for $\nu=0.25$, the difference makes 4.3 %, while, for $\nu=0.20$, the difference of 4.6 %, could be hardly acceptable. In conclusion, it can be stated that the single-spring model may be applied to particular loading cases. However, for complex shapes and loading histories a correction of the model could be required.

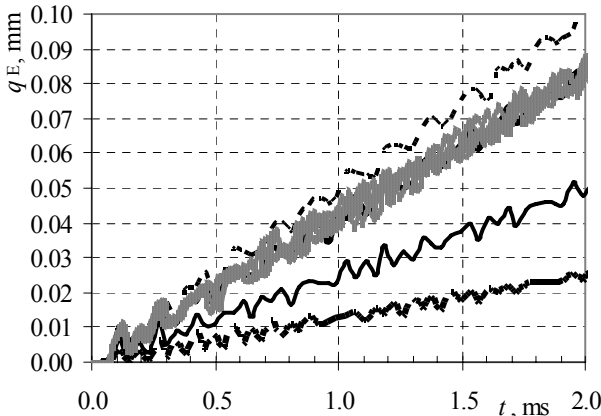


Fig. 6 Time histories of transversal displacement q_E for different values of Poisson's ratio

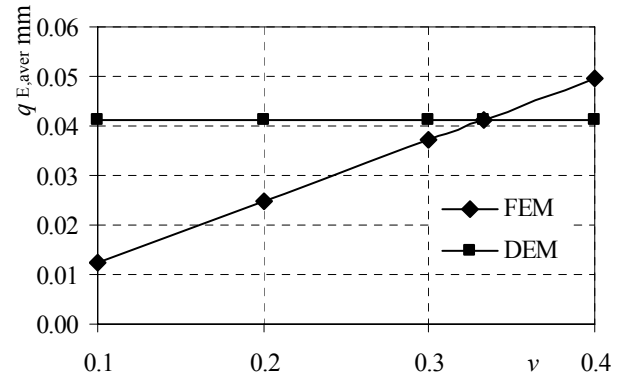


Fig. 7 Variation of average transversal displacement against Poisson's ratio

5. Applications to brittle fracture

The developed single-spring lattice model was implemented into DEM code and was applied to simulate the dynamic behaviour in brittle fracture.

The fracture is considered as brittle rupture of inter-particle connection element $i-j$ under tension. This feature is added to elasticity properties (Fig. 1, c). Formally, it is defined by the condition

$$F_{ij} = R_{ij} \quad (25)$$

The fracture leading to debonding of the neighbouring particles occurs, when the tensile force exceeds the element's load carrying capacity

$$R_{ij}^n = \sigma_0 A_{ij}^{eff} \quad (26)$$

where σ_0 is tensile strength, while

$$A_{ij}^{eff} = \frac{\sqrt{3}}{3} Ls \quad (27)$$

is the effective section area.

When the condition (25) is not fulfilled, i.e. $F_{ij}^n < R_{ij}^n$, the connection element works as a spring and interaction of particles is allowed. When the condition (25) is satisfied, debond (disconnection) of the element occurs and the interelement stiffness is removed from the equation of motion (3). In the case of repeated interaction of particles, i.e.

$$h_{ij}^n \leq 0$$

the connection element is restored again.

The described rectangular plate under compression loading (Fig. 3) will be investigated. Here, the controlled displacement of wall CD will be increased up to 2.5 mm. The elasticity properties are characterized by the elasticity modulus $E = 17.1$ GPa and by the fixed value of Poisson's ratio $\nu = 0.33$.

Two types of tensile strength were examined against fracture. A homogeneous material is characterized by the constant strength value $\sigma_0 = 250$ MPa. A heterogeneous material is defined by the average value

$\sigma_0 = 250$ MPa, while random heterogeneity is governed by Gaussian distribution. Hence, tensile strength values σ_{0ij} of any connection element ij are assumed to be a random parameter, ranging between $(1 - \alpha)\sigma_0 \leq \sigma_{0ij} \leq \sigma_0(1 + \alpha)$ and being generated computationally, using the random number generator. Here, α stands for heterogeneity fraction ($0 \leq \alpha \leq 1$), while their value is assumed to be $\alpha = 0.2$.

A relatively fine grid with the characteristic size $L = 1.6667$ mm was used in fracture analysis. The DEM lattice scheme contains 50640 connection elements, $n = 17076$ nodes and 34152 degrees of freedom.

The possibilities of the DEM are illustrated by the reaction force of the wall AB (Fig. 8).

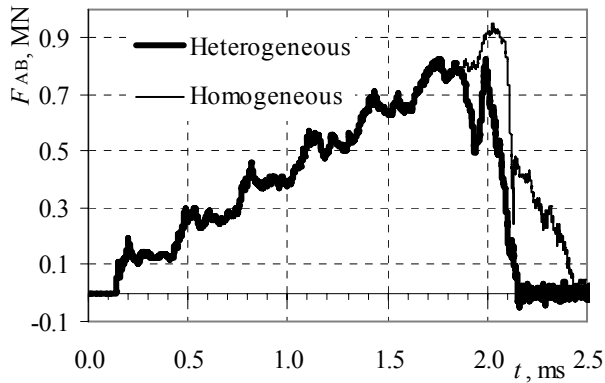


Fig. 8 Time variation of the reaction forces acting on the wall AB

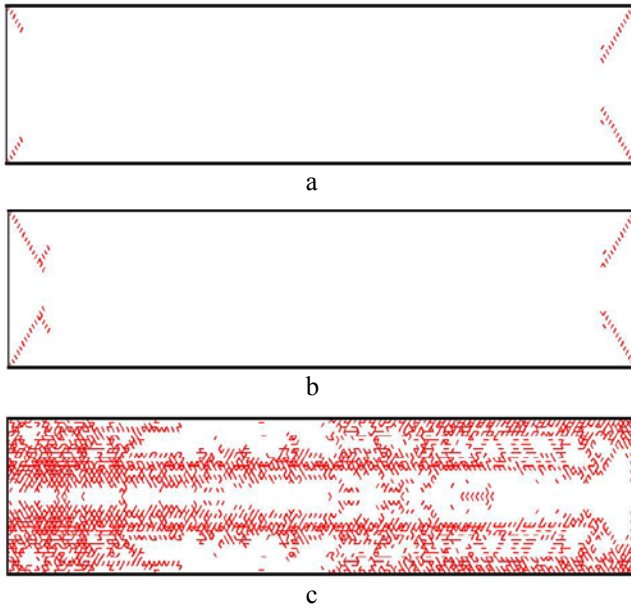


Fig. 9 Cracking pattern of the homogeneous plate at various time moments: a – $t = 1.70$ ms, b – $t = 2.00$ ms, c – $t = 2.30$ ms

The ascending branch illustrates dynamic behaviour of the plate during loading, while the descending branch reflects unloading caused by fracture behaviour. It was found that the first debonding of the connection elements occurred in the vicinity of the imitated defect in the middle of the plate. For a homogeneous plate it occurs at the time moment $t_1 = 1.685$ ms with the failure load value and displacement value, while, for a heterogeneous plate,

the failure occurs at the time instance $t_2 = 1.675$ ms. The delay in Fig. 8 is explained by the time required to move the shock wave from the centre to the support.

The duration of the fracture of the homogeneous plate is 2.5 times shorter compared to that of the heterogeneous plate.

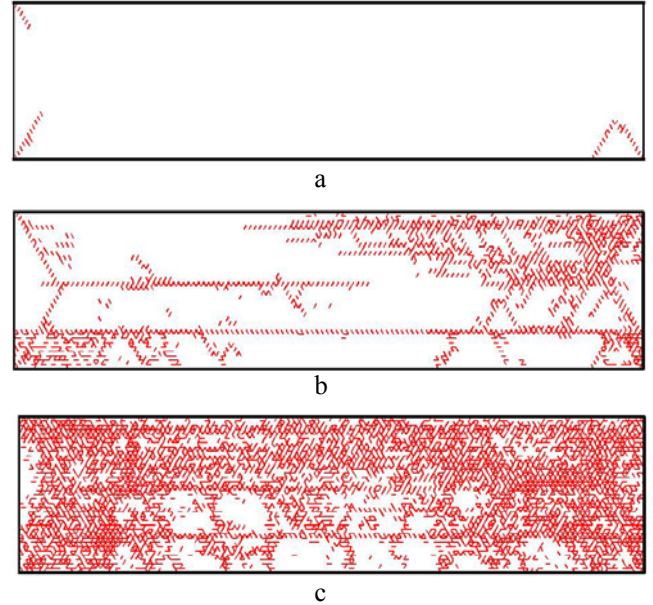


Fig. 10 Cracking pattern of the heterogeneous plate at various time moments: a – $t = 1.70$ ms, b – $t = 2.00$ ms, c – $t = 2.30$ ms

The propagation of cracking from the initial state up to failure is presented in Fig. 9 for the homogeneous plate, and, in Fig. 10, for the heterogeneous plate. Here, debonded connections are shown by thick lines.

The fracture of the homogeneous plate (Fig. 9) is of regular pattern and is symmetric with respect to a longer side (axis Ox). The propagation direction is generally predefined by the lattice geometry. The formation of the regular inclined and normal cracks was detected. The fracture of the heterogeneous plate (Fig. 10) is much more complicated. Multiple cracking of random character and formation of several irregular magistral cracks is observed.

6. Conclusions

The developed continuum consistent single-spring lattice model was applied to DEM simulations and implemented into DEMMAT code.

The model operates using the single-spring stiffness which is a parameter dependent on Poisson's ratio ν . It was observed that longitudinal deformation is practically precisely described independently on the values of Poisson's ratio.

The obtained values of a transverse displacement show that the above model is accurate for the value $\nu = 0.33$, as expected while the occurring differences are asymptotically increasing for other values. Considering the results obtained for the compression plate, it was found that, for the most popular materials with reduced $\nu = 0.25$, the transversal displacements may be obtained with 22% error.

The model was applied to simulation of dynamic fracture of 2D solid plate with random properties. The results obtained show that the method is an effective simulation tool for qualitative investigation of brittle fracture behaviour. It is able to capture naturally occurring multiple cracking patterns with randomly oriented cracks.

References

1. **Cundall, P.A., Strack, O.D.L.** A discrete numerical model for granular assemblies. -*Géotechnique*, 1979, v.29, No.1, p.47-65.
2. **Kawai, T., Kawabata, K. Y., Kondou, I., Kumagai, K. A.** A new discrete model for analysis of solid mechanics problems. -In Proc. of the 1st Conference on Numerical Methods and Fracture Mechanics. 1978, Swansea, p.26-37.
3. **Rena, W.X., Tanb, X., Zheng, Z.** Nonlinear analysis of plane frames using rigid body-spring discrete element method. -*Computers and Structures*. 71, 1999, p.105-119.
4. **Bicanic, N., Stirling, C., Pearce, C. J.** Discontinuous modelling of structural masonry. -Fifth World Congress on Computational Mechanics. July 7-12. Vienna. Austria. 2002, p.1-18.
5. **D'Addetta, G.A., Ramm, E.** A microstructure-based simulation environment on the basis of an interface enhanced particle model. -*Granular Matter*. 8, 2006, p.159-174.
6. **Procházka, P.P.** Application of discrete element methods to fracture mechanics of rock bursts. -*Engineering Fracture Mechanics*. 71, 2004, p.601-618.
7. **Hunt, S. P., Meyers, A. G., Louchinikov, V.** Modelling the Kaiser effect and deformation rate analysis in sandstone using the discrete element method. -*Computers and Geotechnics*. 30, 2003, p.611-621.
8. **Hentz, S., Donzé, F. -V. and Daudeville, L.** Discrete element modelling of concrete submitted to dynamic loading at high strain rates. -*Computers and Structures*. 82, 2004, p.2509-2524.
9. **Khanal, M., Schubert, W., Tomas, J.** DEM simulation of diametrical compression test on particle compounds. -*Granular Matter*. 7, 2005, p.83-90.
10. **Thorton, C., Ciomocos, M. T., Adams, M. J.** Numerical simulations of diametrical compression tests on agglomerates. -*Powder Technology*, 140, 2004, p.258-267.
11. **Vadluga, V., Kačianauskas, R.** Numerical simulation of rupture and energy balance of 1D continuum by using discrete element method. ISSN 1392-1207. -*Mechanika*. Nr.3(59). -Kaunas: Technologija, 2006, p.5-12.
12. **Vadluga, V., Kačianauskas, R.** A simulation of dynamic fracture of tension plate with randomly distributed material properties by discrete element method. -Full papers of the 9th Int. Conf. Held on May 16-18. -Vilnius. Lithuania. CD-ROM. p.1-7.
13. **Ibrahimbegovic, A., Delaplace, A.** Microscale and mesoscale discrete models for dynamic fracture of structures built of brittle material. -*Computers and Structures*, 81, 2003, p.1255-1265.
14. **D'Addetta, G. A., Kun, F., Ramm, E.** On the application of a discrete model to the fracture process of cohesive granular materials. -*Granular Matter*, 4, 2002, p.77-90.
15. **Lilliu, G., Van Mier, J.G.M.** 3D lattice type fracture model for concrete. -*Engineering Fracture Mechanics*, 70, 2003, p.927-941.
16. **Sawamoto, Y., Tsubota, H., Kasai, Y., Koshika, N., Morikawa, H.** Analytical studies on local damage to reinforced concrete structures under impact loading by discrete element method. -*Nuclear Engineering and Design*, 179, 1998, p.157-177.
17. **Mustoe, G.G.W.** A generalized formulation of the discrete element method. -*Engineering Computations*. 9(2), 1992, p.181-190.
18. **Griffiths, D.V., Mustoe, G.G.W.** Modelling of elastic continua using a gillage of structural elements based on discrete element concepts. -*Int. J. for Numerical Methods in Engineering*, 50, 2001, p.1759-1775.
19. **Liu, K., Liu, W.** Application of discrete element method for continuum dynamic problems. -*Archive of Applied Mechanics*, 2006, Vol. 76, No. 3-4, p.1-8.
20. **Liu, K., Gao, L.** The application of discrete element method in solving three-dimensional impact dynamics problems. -*Acta Mechanica Sinica*, 2003, v.16, No.3, p.256-261.
21. **Ricci, L., Nguyen, V.H., Sab, K., Duhamel, D., Schmitt, L.** Dynamic behaviour of ballasted railway tracks: A discrete/continuous approach. -*Computers and Structures*, 83, 2005, p.2282-2292.
22. **Azavedo, N.M., Lemos, J.V.** Hybrid discrete/finite element method for fracture analysis. -*Computer Methods in Applied Mechanics and Engineering*, 195, 2006, p.4579-4593.
23. **Džiugys, A., Peters, B.** An approach to simulate the motion of spherical and non - spherical fuel particles in combustion chambers. -*Granular Matter*, 3, 2001, p.231-265.
24. **Balevičius, R., Džiugys, A., Kačianauskas, R.** Discrete element method and its application to the analysis of penetration into granular media. -*J. of Civil Engineering and Management*, 2004, 10(1), p.3-14.
25. **Balevičius, R., Kačianauskas, R., Džiugys, A., Maknickas, A., Vislavičius, K.** Investigation of performance of programming approaches and languages used for numerical simulation of granular material by the discrete element method. -*Computer Physics Communications*, 175(6), 2006, p.404-415.
26. **Moaveni, S.** Finite Element Analysis. Theory and Applications with ANSYS -Saeed Moaveni, Prentice Hall, Upper Saddle River. -New Jersey 07458, 1999.-527p.

V. Vadluga, R. Kačianauskas

DVIMAČIO KŪNO MODELIAVIMAS DISKREČIŲJŲ ELEMENTŲ METODU TAIKANT VIENOS SPYRUOKLĖS TINKLELĮ

R e z i u m ė

Šiame darbe nagrinėjama tamprus dvimačio kūno dinaminis modeliavimas diskrečiųjų elementų metodu (DEM). Diskretinis modelis sudarytas iš šešiakampio tinklelio. Spyruoklės standumo koeficiento priklausomybė nuo Puasono koeficiento išvesta virtualiųjų poslinkių metodu.

Pasiūlyto modelio tinkamumas patikrintas gautus rezultatus lyginant su BEM rezultatais. Parodytas šio modelio tinkamumas trapijam irimui modeliuoti. Čia kaip pavyzdys pasirinkta gniuždoma plokštelė su atsitiktinai pasiskirsčiusia stiprumo riba. Dinaminio irimo procesas pa-vaizduotas yrančios plokštelės vaizdais atskirais laiko momentais. Gauti irimo vaizdai palyginti su vienalytės medžiagos rezultatais.

V. Vadluga, R. Kačianauskas

INVESTIGATION OF THE SINGLE-SPRING LATTICE MODEL IN SIMULATION OF 2D SOLID PROBLEMS BY DEM

S u m m a r y

Simulation of the elastodynamic behaviour of two-dimensional solid is considered by the Discrete Element Method (DEM). The discrete approach is implemented in the form of the hexagonal lattice. The single-spring model yielding Poisson's ratio dependent stiffness was derived by the virtual displacement method. Suitability of the suggested model was verified by comparing it with the FEM results. The application of the model to brittle fracture is demonstrated. Cracking of the plate under compression with randomly distributed tensile strength properties of the material is considered as a case study. The dynamic fracture behaviour is illustrated by time variation of forces and the cracking pattern of the element network.

The results obtained are compared with the behaviour of a homogeneous plate.

В. Вадлуга, Р. Качанаускас

МОДЕЛЬ РЕШЕТКИ С ЕДИНСТВЕННОЙ ПРУЖИНОЙ ДЛЯ ОПИСАНИЯ ДВУХМЕРНЫХ СРЕД МЕТОДОМ ДИСКРЕТНЫХ ЭЛЕМЕНТОВ

Р е з ю м е

Рассматривается моделирование упругого динамического деформирования двухмерной среды методом дискретных элементов (МДЭ). Дискретная модель представлена в форме гексагональной решетки. Модель единственной пружины, приводящей к параметру жесткости, зависящему от коэффициента Пуассона, выводится методом виртуальных перемещений. Предложенная модель проверена сопоставлением с результатами расчёта по МКЭ. Далее метод применен для моделирования хрупкого разрушения пластины. Пластина с неоднородным случайным распределением предела прочности на растяжение, рассматривается в качестве примера. Динамический характер разрушения иллюстрируется временным изменением опорной реакции, а так же структуры разрушения. Результат расчёта неоднородной пластины сравнивается с результатами расчёта однородной пластины.

Received August 30, 2007